Temporal coding in the auditory brainstem of the barn owl

J. Z. Simon[1], S. Parameshwaran[2], T. Perney[3] and C. E. Carr[2]

[1]Institute for Systems Research and [2]Department of Biology, University of Maryland, College Park, Maryland, 20742, USA and [3]Institute for Neuroscience, Rutgers University, New Jersey, 07102 USA
cc117@umail.umd.edu

1. Introduction

In birds and mammals, precisely timed spikes encode the timing of acoustic stimuli, and interaural acoustic disparities propagate to binaural processing centers such as the avian nucleus laminaris (NL) and the mammalian medial superior olive (MSO; Young & Rubel, 1983; Carr & Konishi, 1990; Smith et al., 1993). The projections from the cochlear nucleus magnocellularis (NM) to NL and from mammalian spherical bushy cells to MSO resemble the Jeffress model for encoding interaural time differences (Jeffress, 1948). The Jeffress model has two fundamental elements: delay lines and coincidence detectors. A Jeffress circuit is an array of coincidence detectors, every element of which has a different relative delay between its ipsilateral and contralateral excitatory inputs. Thus the interaural time difference (ITD) is encoded into the position (a place code) of the coincidence detector whose delay lines best nullify the acoustic ITD. The neurons of NL and MSO phase-lock to both monaural and binaural stimuli. They respond maximally when phase-locked spikes from each side arrive simultaneously, i.e. when the difference in the conduction delays is nullified by the ITD (Goldberg & Brown, 1969; Yin & Chan, 1990; Carr & Konishi, 1990; Overholt et al., 1992; Peña et al., 1997).

Several specializations have been identified that allow preservation and enhancement of temporal information in NL and NM cells. The end bulbs of Held provide a morphological substrate for the preservation of the time information between the auditory nerve and the neurons of NM (Jhaveri and Morest 1992b; Parks and Rubel, 1975). At the molecular level, an abundance of AMPA receptors expressed postsynaptically contribute to the short duration of the excitatory postsynaptic potentials (EPSPs) by virtue of their rapid desensitization kinetics (Raman et al., 1994). In addition to the configuration of synaptic inputs, the temporal firing pattern of a neuron is largely determined by its intrinsic membrane conductances. Of particular interest are the voltage sensitive K^+ conductances. The importance of K^+ channels in sculpting the response properties of auditory neurons was first demonstrated by Manis and Marx (1991). They showed that differences in the electrical responses of bushy cells and stellate cells in the mammalian cochlear nucleus may be attributed to a distinct complement of outward K^+ currents in each cell type.

Different K^+ channels shape the temporal firing pattern of auditory neurons (Brew and Forsythe, 1995; see Trussell, 1999; Oertel, 1999 for reviews). Because knowledge of channel abundance and distribution is necessary for understanding the role of voltage sensitive conductances in temporal coding, we have examined the

expression of the Shaw-like potassium channel Kv3.1, a delayed rectifier with a high threshold of activation. We have also implemented a model of a NL neuron that pays special attention to the roles of fast K^+ channels. The model also examines the roles of multiple dendrites, rate coding vs. phase-locked coding, spike initiation in thresholding, and non-phase-locked depolarizing inhibition. All of these may play crucial roles for *in vivo* coincidence detection, and thus for *in vivo* sound localization.

2.1 Expression of potassium conductances in the auditory brainstem

High levels of Kv3.1 immunoreactivity characterize both NM and NL in the barn owl. In NM, the majority of Kv3.1 immunoreactivity appears perisomatic. Cells in NM that encode high best frequency (BF) sounds show intense immunoreactivity (Figure 1). The expression levels diminish gradually with lower BF neurons displaying a prominent gradient in Kv3.1 level. The neuropil in and around NM is moderately stained, and the axons and dendrites are indistinguishable from each other. Unlike the high and mid BF regions, the very low BF region of NM is made up of stellate cells that receive bouton terminals from the auditory nerve (Köppl, 1994). These low BF cells express very low levels of Kv3.1.

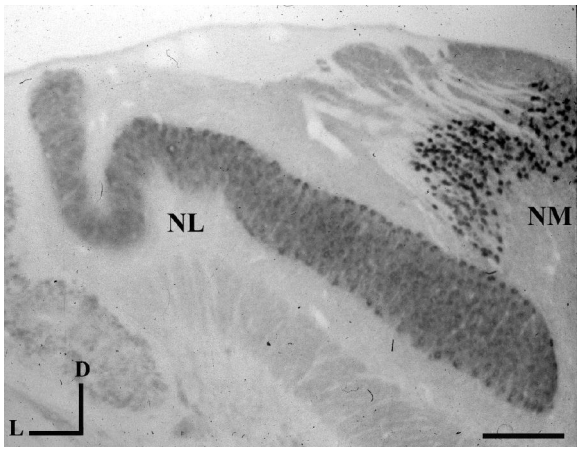

Figure 1. Kv3.1 in the time coding nuclei of the auditory brainstem of the barn owl. Note high levels of Kv3.1 immunoreactivity in both NM and NL. NM= nucleus magnocellularis, NL = nucleus laminaris, D= dorsal, L= lateral, Bar =500µm.

Kv3.1 immunoreactivity in owl NL is characterized by dense staining of the whole structure (Figure 1). Putative NM terminals form intensely immunoreactive puncta that outline each NL neuron, leaving a faintly immunoreactive center. The NM axons that comprise the neuropil surrounding the NL cells are moderately immunoreactive. In the low BF region of NL, the intensity of staining in these perisomatic profiles is reduced, demonstrating the same gradient in Kv3.1 level along the tonotopic axis as observed in NM. The NM axons and the dendrites of NL that make up the neuropil around the neurons of NL also contribute to the observed gradient in Kv3.1 expression along the tonotopic axis. Thus, in the brainstem auditory nuclei, Kv3.1 appears to be expressed at high levels in the presynaptic delay line terminal arbors. It may also occur in the postsynaptic dendrites of NL neurons. Kv3.1 may therefore contribute to the ability of NM to relay temporal information to NL.

2.2 A model of coincidence detection

A biophysically detailed model constructed in the NEURON programming environment (Hines & Carnevale, 1997) investigates the cell's ability to detect coincidences between ipsilateral and contralateral inputs from NM. The role of dendritic processing is explored and emphasized, including the effects of: active potassium channels in the dendrites on spike rate and phase-locking, dendrite size on EPSPs, synaptic reversal potentials on EPSPs, synaptic distribution along the dendrites, and parallel (multiple) dendritic processing. The model makes several predictions, some which confirm those of a previous model (Agmon-Snir et al., 1998): Low voltage activated (LVA) potassium channels greatly increase the ability to detect coincidences at high frequencies; The most efficient dendritic length decreases with BF; Rate-coded output is much more robust than vector-strength-coded output at distinguishing coincidences from partial coincidences; The phase locking of the output spikes is sharper than the phase locking of the synaptic inputs; The required densities of LVA potassium channels are significant, but substantially smaller than those found experimentally in vestibular neurons; There is an optimal number of dendrites for a given stimulus frequency, dendritic length, and number of synaptic inputs; Ceiling effects from the synaptic reversal potential decrease the rate of false detections.

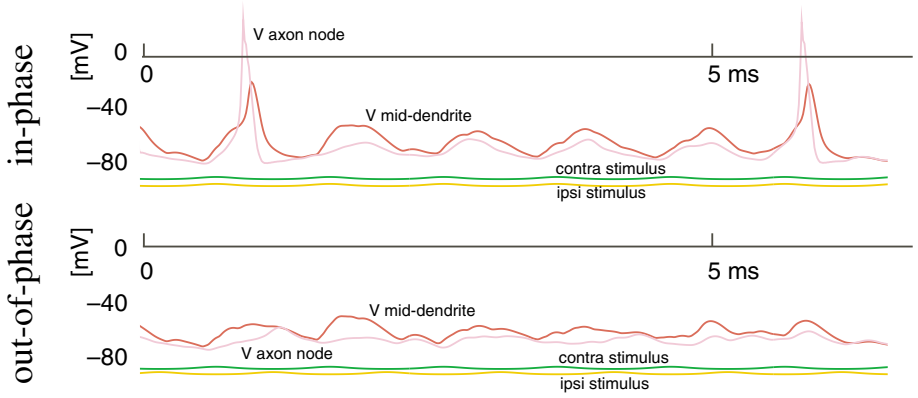

Figure 2. The intracellular potential in model cells as function of time at the axon's first node of Ranvier and the middle of one dendrite. The two graphs demonstrate the same cell receiving continuous 1 kHz stimuli: the upper graph binaurally in-phase, and the lower graph binaurally out-of-phase. When the intracellular potential at the node of Ranvier crosses a spike-counting threshold (usually –35 mV), a spike is counted. The acoustic stimuli are also displayed for reference.

The anatomical and physiological parameters describing the model cells are taken from the literature: from NL physiology when possible, and from nuclei believed to have similar properties (e.g. NM) when not (see below for specific examples). The model automatically generates physiologically useful statistics such as spike rate and vector strength, in both numerical and graphical forms. Each model neuron is constructed from the following sections: multiple dendrites, a soma, an axon hillock, a myelinated segment, and a node of Ranvier. Each section has multiple discretized compartments, and passive conductance in addition to any voltage-dependent conductances.

Acoustic stimuli are turned into neural inputs in two steps. First a probability density function is constructed with the same frequency and phase as the acoustic stimulus, with amplitude normalized to the appropriate value for the incoming EPSP rate (~350 EPSPs/s/synapse; Reyes et al, 1996). Then individual EPSPs are randomly

released via an inhomogeneous Poisson process (with some dead time) with the above time-dependent probability amplitude, in the form of an alpha function conductance.

The number, length, and branching of real NL dendrites varies tonotopically (from low to high BF) from 2 to 20, from 20 μm to 400 μm, and from much to little, respectively (Smith & Rubel, 1979). The model demonstrates that number and length of dendrites is critical to coincidence detection, in a frequency dependent manner (that length is critical is also supported by the model of Agmon-Snir et al., 1998) for NL.

The dendritic and somatic sections have low voltage activated (LVA) and high voltage activated (HVA) K^+ conductances (see Oertel, 1999 and Trussell, 1999 for reviews and Manis & Marx, 1991; Rothman et al., 1993; Reyes et al., 1994; Zhang & Trussell, 1994; Brew & Forsythe, 1995; Perney & Kaczmarek, 1997; Rathouz & Trussell, 1998).

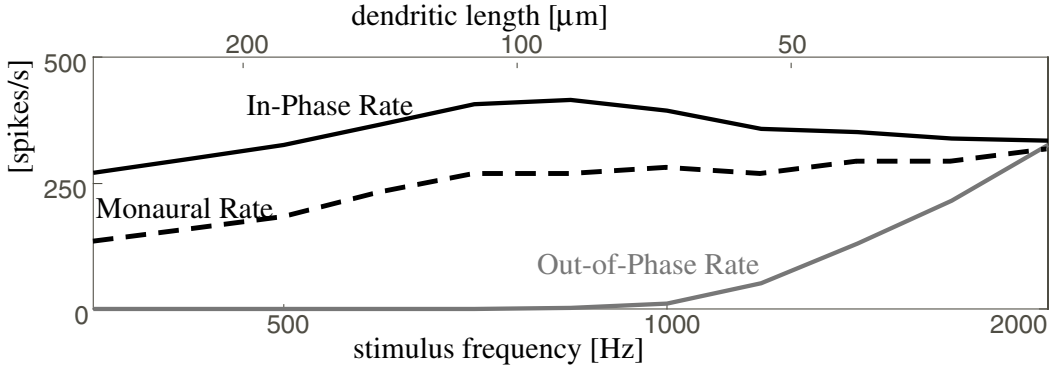

Figure 3. Spike rates compared across a tonotopically arrayed group of model chick NL neurons, each receiving continuous pure tone input at BF. The top curve is the firing rate when the stimuli are in phase, the bottom when the inputs are out of phase. The in-phase firing rate is relatively unchanged from cell to cell, at about 350 spikes/s. The out-of-phase firing rate is almost zero for low BF cells. Starting at ~1 kHz, the cells' ability to discriminate between the in-phase and out-of-phase inputs worsens, failing completely at 2 kHz (primarily due to the poor phase-locking of the inputs to the NL cell, i.e. the outputs of the presynaptic NM cells).

One expects LVA channels to decrease the effective membrane time constant (i.e. the average membrane time constant for a cell receiving and processing *in vivo* rates of EPSPs, which will be much shorter than the passive membrane time constant; Softky & Koch, 1993; Mainen & Sejnowski, 1995). In the model, lowering the density of fast conductances reduces the cell's ability to detect coincidences. The cell's ability to fire with only monaural input and no spontaneous activity on the other dendrite's input is evidence for a new coincidence detection paradigm: out-of-phase subtraction, in addition to the usual in-phase summation (Colburn et al, 1990; Colburn, 1996; Agmon-Snir et al, 1998).

The role of fast LVA K^+ channels can be demonstrated with a monaural input. In Figure 3, the dashed line between the rate curves for in- and out-of-phase is the rate curve for the monaural stimulus. As expected experimentally (Goldberg & Brown, 1969; Yin & Chan, 1990; Carr & Konishi, 1990), the monaural rate, while lower than the binaural in-phase rate, is higher than the binaural out-of-phase rate, even with no spontaneous activity from the opposite side. The model indicates that this is due to LVA K^+ channels, which suppress spike initiation in the out-of-phase case: EPSPs delivered to the soma by one dendrite are subtractively blocked by K^+ conductances in the opposite dendrite, which were activated by its recent (out-of-phase) activity.

The role that HVA K^+ channels play is less clear. Their postsynaptic influence on spike rate and vector strength appears to be minimal in the coincidence detector neuron. Decreasing the conductance from 0.03 S cm^2 to zero does not change either spike rate or vector strength. Increasing the conductance from 0.03 S cm^2 to 3.0 S cm^2 decreases spike rate only moderately and has no effect on vector strength. Presynaptically, Kv3.1 conductance may significantly decrease the width of the presynaptic spike, however, and thus decrease the half width of the EPSC (Kanemasa et al., 1995; Perney and Kaczmarek, 1997; see Sabatini and Regehr, 1999). An increased EPSP width does negatively affect the coincidence detection of a model cell, but only moderately.

The model is primarily one of individual coincidence detection neurons, as opposed to Jeffress-like networks of neurons, but one type of network activity is relevant for the characterization of individual neurons receiving natural inputs: non-phase-locked, inhibitory feedback, e.g. from the avian superior olive. An interesting twist in the NL system is that the inhibition appears to be strongly depolarizing (Hyson et al., 1995; Funabiki et al., 1998; Yang et al., 1999). Diffuse, non-phase-locked inhibition provides automatic gain control by suppressing activity uniformly across a network: the contrast between high-firing rate neurons and low-firing rate neurons is enhanced. Strongly depolarizing inhibition appears contradictory—in this case the inhibitory synaptic reversal potential is above the spike initiation threshold (Funabiki et al., 1998; Yang et al., 1999), but works by both increasing conductance itself and by recruiting the LVA K^+ conductance as well.

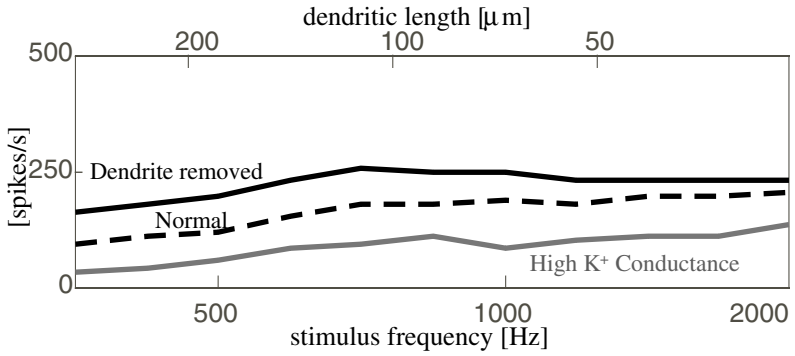

Figure 4. Similar to Figure 3, but a model of barn owl cells (i.e. chick cells but with BF above 4 kHz, multiple short dendrites, and better phase-locking of neuronal inputs from NM (Sullivan & Konishi 1984; Carr & Konishi, 1990). The in-phase firing rate is relatively flat, and the cell's ability to discriminate between the in- and out-of-phase inputs fails completely only at ~ 6 kHz, well above the 2 kHz cut-off of the chick model (but still below the 8-10 kHz expected for barn owl).

3. Discussion

Neurons performing coincidence detection can output the results of their calculation according to several, overlapping coding schemes. The simplest scheme is a rate code, which is used throughout the auditory system, but other schemes which use timing information also exist prominently in the auditory system, most notably in the inputs to the coincidence detector. The computational output of the coincidence detector could be encoded by either spike rate or phase-locking. The cellular mechanisms employed by the model enhance the phase locking of the outputs over that of the inputs. For frequencies with already strongly phase-locked inputs, this effect also

produces enhanced phase locking when the inputs are not in phase, leading to Vector-Strength-IPD tuning curves that are broadly tuned compared to the companion Rate-IPD tuning curves.

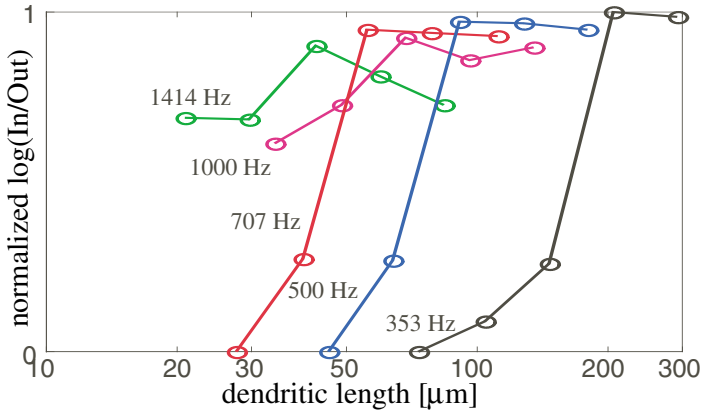

Figure 5. The dendritic gradient used above (Rubel & Smith, 1979) can be predicted by the model (as also by the model of Agmon-Snir et al., 1998). The ratio of firing rate for in-phase stimuli to firing rate for out-of-phase stimuli is plotted against dendritic length for several stimulus frequencies, for chick (the ratio is plotted on a normalized logarithmic scale). For each stimulus frequency, as dendritic length increases, the ability to discriminate between in- and out-of-phase stimuli increases, until a dendritic length is reached for which the ability to discriminate no longer increases. The dendritic length that optimizes the ability to discriminate is a function of stimulus frequency: Optimal dendritic length decreases as frequency increases.

The model shows that there is sufficient experimental data to construct a well-behaved model of chick NL cells. There is less physiological data available from barn owl than from chick (especially channel conductances, voltage dependencies, and kinetics), but without substantial changes, preliminary data shows coincidence detection possible at frequencies up to 6 kHz, without any new specialized structures, but by only fine-tuning mechanisms already present in the chick.

4. Acknowledgements

Supported by NIH DC00436 to CEC and by NIH DC02728 to TP. J. Simon is supported by ONR MURI # N00014-97-1-0501 and NSF # 9720334 to S. Shamma.

5. References

Agmon-Snir H., C. E. Carr and J. Rinzel (1998) The role of dendrites in auditory coincidence detection. Nature *393*:268-272.

Brew H. M. and I. D. Forsythe (1995) Two voltage-dependent K^+ conductances with complementary functions in postsynaptic integration at a central auditory synapse. J Neurosci *15*:8011-22.

Carr C. E. and M. Konishi (1990) A circuit for detection of interaural time differences in the brainstem of the barn owl. J. Neurosci. *10*:3227-3246.

Colburn H. S., Y. Han and C.P. Culotta (1990) Coincidence model of MSO responses. Hear. Res. *49*:335-355.

Colburn H. S. (1996) Computational models of binaural processing. In *Auditory Computation,* H. L. Hawkins, T. A. McMullen, A. N. Popper and R. R. Fay eds. (New York:Springer) 332-400 and references within.

Funabiki K., K. Koyoano and H. Ohmori (1998) The role of GABAergic inputs for coincidence detection in the neurones of nucleus laminaris of the chick. J. Physiol. (Lond) *508.3*:851- 869.

Gamkrelidze G, C. Giaume and K. D. Peusner (1998) The differential expression of low-threshold sustained potassium current contributes to the distinct firing patterns in embryonic central vestibular neurons. J. Neurosci. *18*:1449-1464.

Gerstner W, R. Kempter, J. L. van Hemmen, H. Wagner (1996) A neuronal learning rule for sub-millisecond temporal coding. Nature *383*:76-81.

Goldberg J. M. and P. B. Brown (1969) Response of binaural neurons of dog superior olivary complex to dichotic tonal stimuli: Some mechanisms of sound localization. J. Neurophysiol. *32*:613-636.

Hines M. L. and N. T. Carnevale(1997) The NEURON simulation environment. Neural Computation, *9*:1179-1209. See also <http://www.neuron.yale.edu>.

Hyson R. L., A. D. Reyes and E. W. Rubel (1995) A depolarizing inhibitory response to GABA in brainstem auditory neurons of the chick. Brain Res *677*:117-26

Jeffress L. A. (1948) A place theory of sound localization. J. Comp. Physiol. Psych. *41*:35-39.

Jhaveri S., Morest D. K., (1982) Neuronal architecture in nucleus magnocellularis of the chicken auditory system with observations on nucleus laminaris: a light and electron microscope study. Neuroscience, (4):809-36

Joris P. X., P. H. Smith and T. C. T. Yin (1998) Coincidence detection in the auditory system: 50 years after Jeffress. Neuron *21*:1235-8.

Joseph A. W. and R. L. Hyson (1993) Coincidence detection by binaural neurons in the chick brain stem. J Neurophysiol; *69*: 1197-1211.

Kanemasa T., L. Gan, T. M. Perney, L. Y. Wang and L. K. Kaczmarek (1995) Electrophysiological and pharmacological characterization of a mammalian *Shaw* channel expressed in NIH 3T3 fibroblasts. J. Neurophysiol. *74:207-217.*

Mainen Z. F. and T. H. Sejnowski (1996) Influence of dendritic structure of firing pattern in model neocortical neurons. Nature *382*:363-366.

Manis P. B., Marx S. O. (1991) Outward currents in isolated ventral cochlear nucleus neurons. J. Neurosci 11:2865-2880.

Oertel D. (1999) The role of timing in the brain stem auditory nuclei of vertebrates. Annu. Rev. Physiol. *61*:497-519.

Overholt E. M., E. W. Rubel and R. L. Hyson (1992) A circuit for coding interaural time differences in the chick brain stem. J Neurosci *12*:1698-1708.

Peña J.L, S. Viete, Y. Albeck and M. Konishi (1997) Tolerance to sound intensity of binaural coincidence detection in the nucleus laminaris of the owl. J. Neurosci. *16*: 7046-7054.

Perney T. M. and L. K. Kaczmarek (1997) Localization of a high threshold potassium channel in the rat cochlear nucleus. J. Neurosci.

Rathouz M. and L. Trussel (1998) Characterization of Outward Currents in Neurons of the Avian Nucleus Magnocellularis, J. Neurophysiol. *80*:2824- 2835.

Rothman J. S., E. D. Young and P. B. Manis (1993) Convergence of auditory nerve fibers onto bushy cells in the ventral cochlear nucleus. J Neurophysiol *70*: 2562-83.

Raman I. M., Zhang S., Trussell L. O., (1994) Pathway-specific variants of AMPA receptors and their contribution to neuronal signaling, J Neurosci. *14(8):4998-5010.*

Reyes A. D., E. W. Rubel, W. J. Spain (1994) Membrane properties underlying the firing of neurons in the avian cochlear nucleus. J. Neurosci *14*: 5352-5364.

Reyes A. D., E. W. Rubel, W. J. Spain (1996) *In vitro* analysis of optimal stimuli for phase-locking and time-delayed modulation of firing in avian nucleus laminaris neurons. J. Neurosci *16*: 993-1000.

Sabatini, B. and Regehr, W. (1999) Timing of synaptic transmission. Annu. Rev. Physiol. 61:521-42.

Smith Z.D.J. and E.W. Rubel (1979) Organization and development of brain stem auditory nuclei of the chicken: dendritic gradients in nucleus laminaris. J. Comp. Neurol. *186*:213-239.

Softky W. and C. Koch (1993) The highly irregular firing of cortical cells is inconsistent with temporal integration of random EPSPs. J. Neurosci. *13*:334-350.

Trussell L. O. (1999) Synaptic mechanisms for coding timing in auditory neurons. Annu Rev Physiol 1999;*61*:477-96.

Yang L., P. Monsivais and E. W. Rubel (1999) The superior olivary nucleus and its influence on nucleus laminaris: a source of inhibitory feedback for coincidence detection in the avian auditory brainstem. J. Neurosci. *19*:2313-2325.

Young S. R., Rubel E. W. (1983) Frequency-specific projections of individual neurons in chick brainstem auditory nuclei. J. Neurosci. *7*:1373-1378.

Yin T. C. T. and J. C. K. Chan (1990) Interaural time sensitivity in medial superior olive of cat. J. Neurophysiol. *64*:465-488.

Wang L. Y., Gan L., Forsythe I. D., Kaczmarek L. K., (1998) Contribution of the Kv3.1 potassium channel to high-frequency firing in mouse auditory neurones. J Physiol. 509:183-94

Zhang S. and L. O. Trussell (1994) A characterization of excitatory postsynaptic potentials in the avian nucleus magnocellularis. J. Neurophysiol. *72*:705-718.